Journal of Solid State Electrochemistry (2022) 26:2329–2338
https://doi.org/10.1007/s10008-022-05234-7

ORIGINAL PAPER

Electro-assisted self-assembly of mesoporous silica thin films: application to electrochemical sensing of glutathione in the presence of copper

Farzaneh Asadpour[1] · **Mohammad Mazloum-Ardakani**[1]

Received: 18 February 2022 / Revised: 6 June 2022 / Accepted: 24 June 2022 / Published online: 29 July 2022

Abstract

Oxidation of the reduced form of glutathione based on the 1:1 copper(Cu^{+2})-glutathione(GSH) complexes was found to occur at a decreased overpotential at a glassy carbon electrode modified with highly ordered mesoporous silica thin films (MSTFs) by means of the electrochemically assisted self-assembly (EASA) process. Adsorption of complexes can be performed on the electrode by taking advantage of the anionic nature of the silica walls of the MSTF which provide an excellent fixation site for accumulation of the Cu^{+2}-GSH complex. The current response of voltammetric glutathione sensor is monitored at low oxidation potential of − 0.10 V versus standard mercury/mercurous sulfate reference electrode which makes the proposed sensor applicable to minimize interference from easily oxidizable species in the analysis of biological fluids. The proposed method represents a sensitive voltammetric sensor with a good linear detection range of 1.0–35.0 μM, which is in the range of GSH concentration in physiological fluids reported in literature with a suitable limit of detection of 0.08 μM. The proposed sensor offers several advantages such as being rapid and cost-effective, having good reproducibility, simple operation, and nontoxicity for glutathione detection.

Keywords Voltammetric sensor · Mesoporous silica thin film · Electro-assisted self-assembly method · Copper-glutathione complex · Low overpotential

Introduction

Glutathione, as an auspicious biomarker for early diagnosis of various diseases, has the highest amount of thiol in animal cells with cellular concentrations of 1.0 to 10.0 mM [1]. The antioxidant properties of this tripeptide can act as a sweeper for oxygen-derived free radicals in living systems which are involved in increasing various diseases like diabetes, heart attack, stroke, arthritis, and some types of cancer [2–5]. Glutathione in two forms of reduced and oxidized species supplies the needs of various metabolic processes [6]. In healthy cells and tissue, more than 90% of the total glutathione pool is in the reduced form and less than 10% exists in the disulfide form [7]. A shift in the ratio of these two forms can be an indication of cellular oxidative stress, when glutathione changes from the reduced form (GSH) to the oxidized form (GSSG) [8]. Recently, many studies have shown that alteration in glutathione concentration in human fluids directly leads to several pathological diseases such as diabetes, Parkinson's disease, macular degeneration, HIV disease, and numerous types of cancers [9–11]. For these reasons, the use of sensitive detection methods for monitoring glutathione levels in physiological systems is highly demanded.

Among the available approaches for measuring such thiols, chromatographic measurement techniques [12, 13], capillary electrophoresis/capillary zone electrophoresis (CE/CZE) [14, 15], and flow injection analysis (FIA) [16] present top selectivity and low limit of detection; however, they are time-consuming and costly procedures due to the essential separation/preconcentration steps. Compared to the mentioned techniques, electroanalytical methods [17–20] as less labor-intensive methods for monitoring of thiol have the favorable condition of simplicity and low cost, high detectability and sensitivity, minimal sample pretreatment, and fast responses. The direct oxidation of thiols is slow

✉ Mohammad Mazloum-Ardakani
mazloumardakani@gmail.com

[1] Department of Chemistry, Faculty of Science, Yazd University, Yazd 89195-741, Iran

at usual electrodes and requires a large overpotential about 1.0 V with the problem of electrode passivation [21]. An excellent tactic is to oxidize GSH at lower positive potentials to prevent multiple interferences and background signals as well as electrode fouling. Several amperometric and voltammetric techniques are summarized in Table 1 that benefit from the use of modified electrodes for the electrochemical measurement of glutathione at as low potential as possible.

Recently, there has been interest in the development of electrodes modified with highly arranged mesoporous silica thin films (MSTFs) with nanopore channels produced through the successful electro-assisted self-assembly (EASA), a simple and adaptable method that combines the electrochemical assembly of surfactants at the surface of electrodes by hydrolytic polycondensation of alkoxysilane precursors [22–24]. MSTFs have excellent properties that make them an attractive possibility to use in electrochemical sensing or biosensing. Such deposited films on the electrode by altering the surface demonstrate the beneficial properties of ordered mesoporous materials, including large surface area, narrow pore size distribution, widely open uniform pore structure, obtaining the great fixation site with easily available active place and hosting capabilities for active biomolecules species, high surface area, simple functionalization, and chemical inertness [25, 26]. In addition, the silica films increase the surface area which causes the number of reactive sites to increase, and thus improves the response of voltammetry, which results in an increase in the signal-to-noise ratio. Another advantage of these films is that they can decrease surface passivation [27] by limiting access to the electrode surface; therefore, the thiol is not able to adsorb the electrode metal surface [17].

In our previous work, we have demonstrated that a large amount of the organo-functional groups on the surface of the MSTFs provided a way to capture the gating molecules in order to close the mesopores, which were uncapped using target (insulin) as external stimuli [28]. In this study, the main success of the MSTF application is due to the anionic nature of the silica film walls (silanol group), which provides an excellent fixation site for the accumulation of the Cu^{+2}-GSH complex compound. Indeed, the electrostatic interactions between a positively charged complex ion and the negatively charged silica wall (as a result of the deprotonated silanol groups on the silica surfaces after surfactant extraction from the MSTF at EtOH/HCl solution [25, 29]) contribute to the accumulation of the Cu^{+2}-GSH complex in the film channels and the appearance of an electrochemical redox probe signal after the extraction of surfactant template. To the best of our knowledge, no reports of electrodes decorated with MSTF using the simple EASA technique have been reported for the determination of glutathione, a less electroactive species in the presence of a Cu^{+2} catalyst. This assay provides the detection of glutathione in a cost-effective and a notable way for shortening the time and for easy operation without the complicated pretreatment steps.

Table 1 Electrochemical approaches for the electrochemical determination of glutathione that has already been reported

Electrode	Modification	Method	LDR (μM)	LOD (μM)	Ref
GC	Enzyme/Os-PVP	CV	1–200	0.5	[43]
GC	SWCNT/TOQ	CV	0.07–500	0.07	[44]
GC	CoTSPc-PLL	CV	0.05–2.16	0.02	[45]
GC	Hg(II)-DPTA-Pb(II)	DPV	0.032–32.5	0.032	[46]
CP	TiO_2-ferrocene carboxylic acid	DPV	0.1–12	0.1	[47]
BPPG	MWCNT/FeT4M PyP	SWV	$1.5–5\times10^3$	0.5	[48]
SP	Catechol	CV	0–60	0.11	[49]
CP	2,7-bis(ferrocenyl ethyl) fluoren-9 one	CV	$52.9–4.19\times10^3$	14	[50]
ABPP	No	CV	100–280	10	[51]
Au	MWCNT	CV	$99–8.8\times10^3$	99	[52]
SP	Prussian blue	CV	2–500	2.0	[53]
CP	TTF-TCNQ	CV	5–340	0.3	[54]
GC	No	CV	1–10	0.14	[34]
GC	Mesoporou silica thin films	CV	1–35	0.08	This work

GC glassy carbon, *CP* carbon paste, *SP* screen-printed, *BPPG* basal plane pyrolytic graphite, *ABPP* acetylene black-packed powder

CV cyclic voltammetry, *SWV* squarewave voltammetry, *DPV* differential pulse voltammetry, *LOD* limit of detection, *LDR* linear dynamic range

SWCNT single-walled carbon nanotubes, *MWCNT* multi-walled carbon nanotubes, *Os-PVP* osmium-polyvinyl pyridine, *TOQ* synthetic triptycene orthoquinone, *TTF-TCNQ* tetrathiafulvalene-tetracyanoquinodimethane, *CoT-SPc-PLL* cobalt tetra sulfonated phthalocyanine immobilized in poly (L-lys), *FeT4MPyP* Fe(III) tetra-(*N*-methyl-4-pyridyl)-porphyrin

Experimental

Chemicals and materials

Copper(II) nitrate trihydrate ($Cu(NO_3)_2.3H_2O$, 99%), glutathione (GSH, 98%), and cysteine (97%) were purchased from Sigma-Aldrich. Tetraethyl orthosilicate (TEOS, 98%, Sigma-Aldrich), ethanol (95 – 96%, Merck), $NaNO_3$ (98%, Acros), and cetyltrimethylammonium bromide (CTAB, 99%, Merck) were utilized for film formation. Potassium hexacyanoferrate (98%, Aldrich), potassium nitrate (KNO_3, 99%, Sigma-Aldrich), and KCl (99%, Acros) were employed as supporting electrolytes. Deionized water (conductivity 18 MQ) and degassed water with N_2 was used to prepare all samples.

Apparatus

All galvanostatic/potentiostatic analyses were measured utilizing a Micro Autolab (Eco Chemie Utrecht, Netherlands). The pH measurements were performed with a Metrohm model 691 pH/mV meter. A routine three-electrode cell system consisting of a standard mercury/mercurous sulfate electrode (MSE, [Hg/Hg2SO4, saturated K2SO4], + 0.64 V vs. standard hydrogen electrode) as the reference electrode, a platinum foil as the counter electrode, and the glassy carbon electrode ($A = 0.0314\,cm^2$, Azar Electrode Co., Urmia, Iran) as a working electrode was used. A transmission electron microscopy (TEM) image of the silica thin film was attained on a Tecnai G^2 F20-ST from FEI Company (U.S.A) operating at 200 kV.

Electrogeneration of the mesoporous silica films on the electrode surface

Electro-assisted deposition of the silica thin film was accomplished using GCE polished with 0.3 and 1.0 µm alumina followed by sonication in water and drying with nitrogen. For film generation, a typical sol includes 20 mL of ethanol and 20 mL of an aqueous solution of 0.1 M $NaNO_3$ while 100 mM TEOS (450 µl) and 32 mM CTAB (0.25 g) were added under stirring [24]. The pH of the mixture was fixed at 3.0 by the addition of 0.1 M HCl. Sol began to hydrolyze by stirring for 2 h under ambient conditions before use. Finally, the silica film was deposited on the surface of the GCE through galvanostatic conditions using a negative current of 0.023 mA cm^{-2} to the electrode immersed in the hydrolyzed solution (TEOS + CTAB) for 40 s (applying a stainless-steel rod as a counter electrode and a silver wire as a pseudo reference electrode). Then, the electrode was immediately pulled out from the sol and washed with water. After film generation, the electrode was kept for one night at 50 °C. The template was removed from the silica film matrix while the electrode was soaked in 0.1 M HCl-ethanol (volume ratio the is 1:9) solution for 6 min under gentle stirring.

Procedure

Schematic 1 summarizes the sensor fabrication steps and the strategy for electrochemical detection of glutathione. The silica film formation was done in one step by using the electrochemically assisted self-assembly EASA approach at electrode surfaces. A negative current is applied to an electrode dipped in an alcoholic solution consisting of a hydrolyzed tetraalkoxysilane Si(OR)4 (R = Et (TEOS) as a source of silicate and CTAB surfactant as a template which leads to the self-assembly of CTAB on the surface of the electrode and TEOS co-condensation. A solution containing a predetermined amount Cu(II), glutathione, and 0.1 M KNO_3 was mixed actively for 5 min to form a Cu^{+2}-GSH complex prior to electrochemical measurement. The silica thin film/GCE was then dipped into this solution for 3 min. The electrostatic interactions between a positively charged complex ion and the negatively charged silica surface originating from surface silanolate groups contribute to the accumulation of the Cu^{+2}-GSH complex compound in the film. Stable cyclic voltammetry (CV) was observed from − 0.4 to + 0.1 Volt versus MSE reference after the third scan. The Cu^{+2}-GSH complex formation was confirmed via IR, UV–visible spectroscopy, and cyclic voltammetry.

Results and discussion

Characterization of the MSTF structure by TEM and FTIR

TEM was used to examine the morphology of the film structure to show the highly ordered and homogeneous film porosity (see top (A) and cross-sectional (B) views in Fig. 1). The morphology of the film structure indicates that the mesochannels are thickly arranged in a typical honeycomb configuration with nanometer vertical channels and a uniform pore size of about 3 nm [22, 26] Scheme 1.

The sharp vibrational band of the Si–O-Si in the range 1070 and 1220 cm^{-1} (Fig. S1) are in good agreement with the formation of a dense network of silica [30]. In addition, a pure silica contains three strong peaks around 3535, 3680, and 3747 cm^{-1}[31]. The latter is a result of silanol groups while the first two peaks are due to hydrogen-bonded water molecules. Therefore, these remarkable peaks were hidden by a broad -OH stretching vibration peak between 2500 and 3500 cm^{-1}[32].

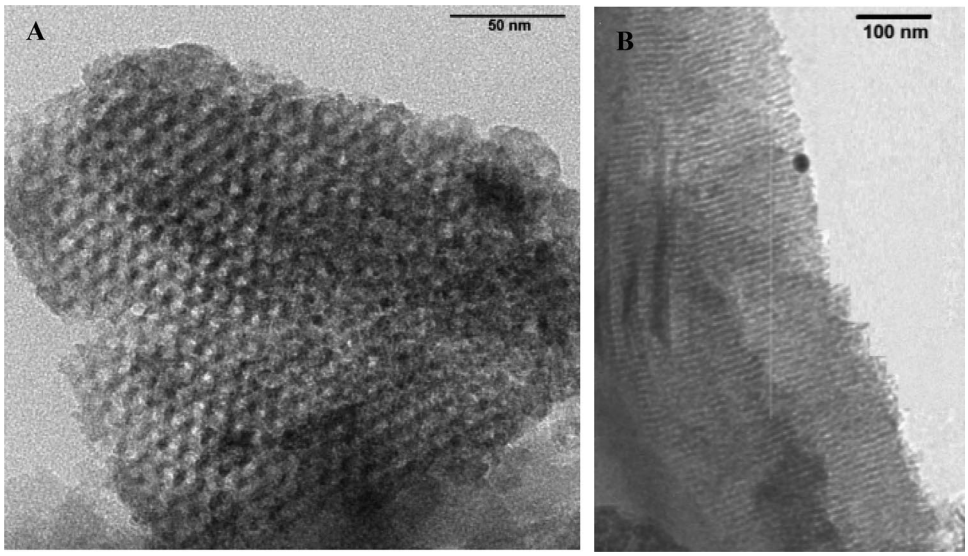

Fig. 1 TEM images of top (**A**) and cross-sectional view (**B**) of silica thin film deposited on modified GCE generated by EASA method

Using anionic redox probe to investigate the presence of the MSTF on the GC electrode

Mass transport issue at the electrode modified with silica film was investigated by cyclic voltammetry using an anionic $Fe(CN)_6^{3-}$ redox probe in Fig. 2. First, before template extraction (curve b), no redox peaks were observed since the films are completely impassable to $Fe(CN)_6^{3-}$ redox probes, confirming that a uniform crack-free silica is deposited on the entire electrode surface. After removing the pattern (curve c), a couple of reversible peaks was observed because the film became porous, allowing the electrochemical probe to diffuse to the electrode surface. However, we found a significant reduction in the electrochemical signal intensity which is comparable to the bare electrode in curve (a) due to some repulsion to mass transport of $Fe(CN)_6^{3-}$ anions as a result of negatively charged silica surfaces. Indeed, the deposited silica film onto the surface of the electrode acts as a barrier that prevents diffusion of $Fe(CN)_6^{3-}$ probe from the solution toward the surface of the electrode. These results well prove the formation of silica film on the electrode surface. Conversely, the accumulation of cationic species, for example, $Ru(bpy)_3^{2+}$ or paraquat, increases the intensity of the electrochemical signal based on previously reported evidence [24].

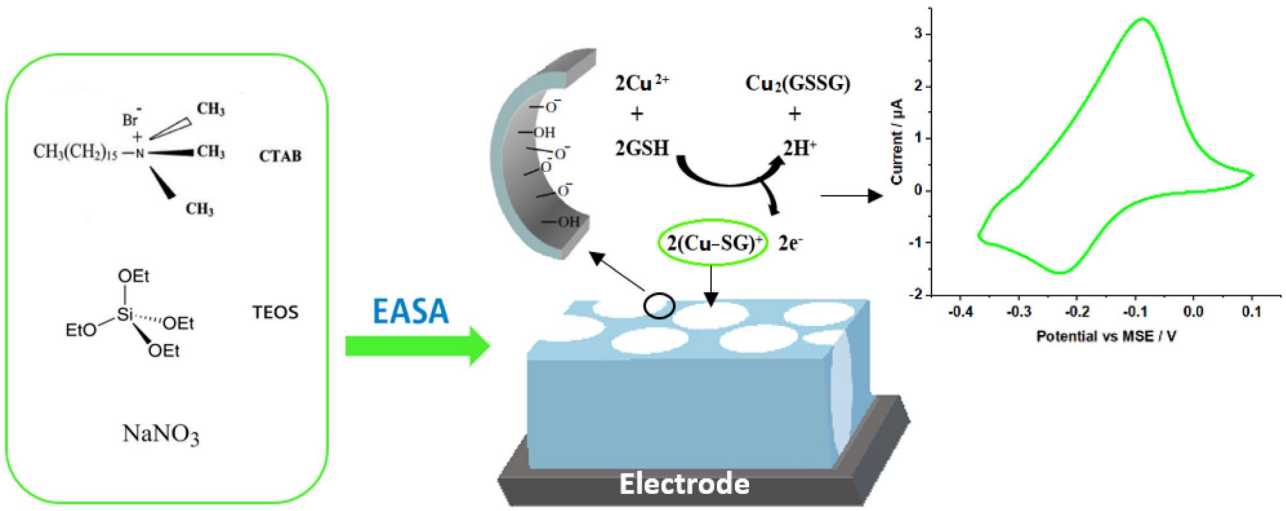

Scheme 1 Schematic illustration of the electrochemical assembly method for the generation of the MSTF on the GC electrode to provide a surface that allows the oxidation of the Cu^{2+}-GSH complex

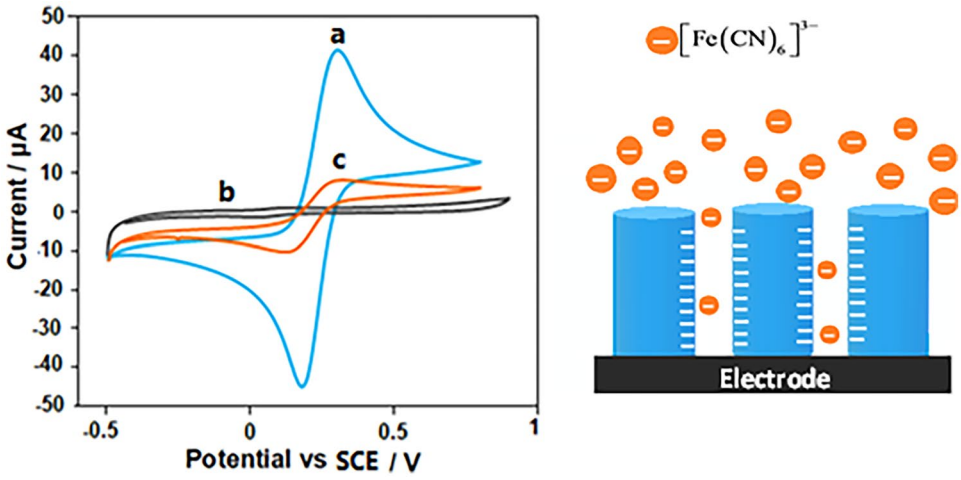

Fig. 2 Cyclic voltammograms obtained with 5 mM $Fe(CN)_6^{3-}$ in 0.1 M KNO_3 (pH 6.0) on (**a**) bare GC electrode, GC electrode modified with a thin mesoporous film (**b**) before and (**c**) after surfactant extraction. Scan rate was 100 mV s^{-1}. Schematic shows that the deposited silica film onto the surface of electrode acts as a barrier that prevents diffusion of $Fe(CN)_6^{3-}$ probe from the solution toward the surface of electrode

The electrochemical oxidation of GSH in the absence and presence of Cu^{+2} species

Figure 3 shows the cyclic voltammograms recorded using glassy carbon electrodes at a potential sweep rate of 50 mV s^{-1} in 0.1 M KNO_3 at two different steps in the absence and presence of copper. After producing a thin film of silica with CTAB surfactant as a template on the surface of the electrode, the voltammetric response was completely suppressed (curve b, on Fig. 3), proposing the MSTF was perfectly deposited on the entire surface of the electrode. The increase of current in the observed signal of curve c after removing the template confirmed the film

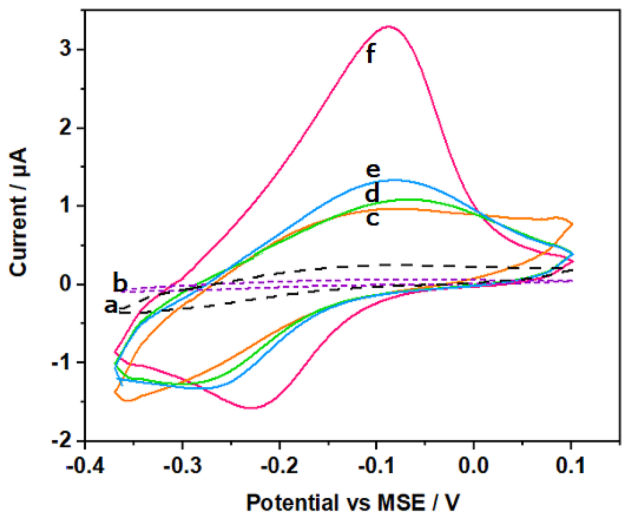

Fig. 3 Cyclic voltammograms of (**a**) bare GC electrode in 0.1 M KNO_3 solution (pH 6.0), (**b**) electrode deposited with MSTF templated with surfactant, (**c**) after template removal from silica films. (**d**) 0.1 M KNO_3 + 35.0 µM Cu^{+2}, (**e**) 0.1 M KNO_3 + 22.0 µM GSH, and (**f**) 0.1 M KNO_3 + 35.0 µM Cu^{+2} ion + 22.0 µM glutathione. Scan rate was 50 mV s^{-1}

became highly porous to electrolyte diffusion. A small anodic peak that arises at − 0.1 V (curve d) corresponds to the oxidation of Cu^{+2} ion, which is not stable under the experimental conditions. Curve e, the blue line in Fig. 3, shows a cyclic voltammogram obtained for 22.0 µM glutathione in the absence of Cu^{+2} ion in 0.1 M KNO_3 solution. It can be observed that during an anodic scan at − 0.1 V *vs.* MSE, the current increased slightly which was related to the oxidation of GSH to GSSG. The direct oxidation of GSH is probably responsible for this slight increase in current. Direct oxidation of thiols is common to give the corresponding disulfides on a carbon electrode through the equation; $2RSH \rightarrow RSSR + 2H^+ + 2e^-$. A significant increase in the GSH oxidation signal (curve f, pink line) on the MSTF-modified electrode was observed for 22.0 µM glutathione in the presence of 35.0 µM Cu^{+2} in 0.1 M KNO3 solution, suggesting that the oxidation of GSH is mediated by copper(II) [33]. In addition, the observation clearly shows the Cu^{2+} requirement for GSH oxidation at the electrode, because a very small signal was observed in the absence of Cu^{2+} for dissolved GSH. Moreover, the silica film by modifying the surface of the electrode increases the surface area, providing a fixation site that contributes to the accumulation of the Cu^{+2}-GSH complex on the silica film due to the electrostatic interaction between the negative charge on the silica surface and positive charge related to the complex. Repetitive cyclic voltammetry was used in order to accumulate Cu^{+2}-GSH complex at modified electrodes with a silica film matrix. Peak current as a function of the number of CV scans was plotted (data not shown). Maximum stable response by cyclic voltammetry was observed after the third scan. Therefore, all the results were shown from the third cycle.

In addition, the result of UV–visible spectroscopy supports the formation of a complex between Cu^{+2} ions and glutathione (Fig. 4). The obvious absorption peak recorded around 300 nm in the spectra after adding glutathione to

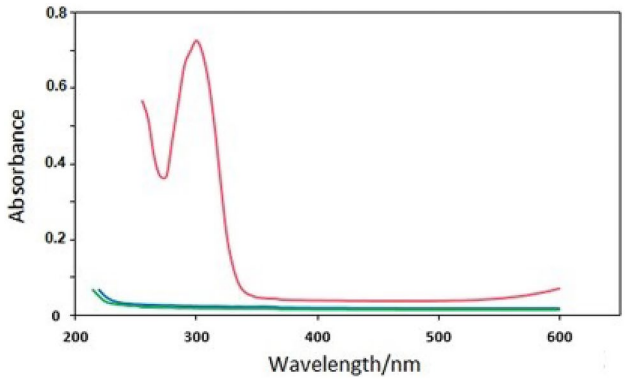

Fig. 4 UV–vis spectra of 0.1 mM Cu^{2+} (green); 0.6 mM GSH (aq) (blue); and 0.6 mM GSH and 0.1 mM Cu^{2+} (aq) (pink) as composition of measured solution after mixing for 15 min (0.1 M KNO_3 solution is blank)

a solution of Cu^{+2} ions is related to the formation of the Cu^{2+}-GSH complex [34]. This result arises from the creation of the copper ion–GSSG complex which does not have a strong absorption in this long-wavelength UV region, where strong absorption of the Cu^{2+}-GSH complex is observed [35]. Moreover, the infrared-active mode assigned to – SH stretching (about 2500 cm^{-1}) for GSH has apparently disappeared in the spectrum of the Cu^{2+}-GSH complex, indicating the formation of the covalent bonds between GSH and Cu^{+2} ions as shown in Fig. S2 [36]. In contrast, the injection of Cu^{+2} ions into the GSSG solution reduces absorption as Areias et al. [34] indicated.

The optimization of pH

Due to the presence of hydroxyl, carboxyl, and amine groups in glutathione, pH is an important parameter that must be considered. Hydrogen bonding is mostly responsible for the aggregation of glutathione, which reduces the possibility of covalent bonding between GSH and Cu^{+2} ions. Therefore, to decrease the possibility of glutathione aggregation, the best condition is when the glutathione molecule is available in the form of zwitterions, which can be attributed to the electrostatic repulsion between negatively charged carboxylic groups in the form of zwitterions (NH^{+3}/COO^{-}/SH/COO^{-}) [37]. As shown in Fig. S3, the maximum voltammetric signal of glutathione is recorded at pH 6, which no aggregation can be induced at this selected pH. In an acidic environment, the carboxylic groups are in protonated form and the aggregation of glutathione could be induced. Moreover, the surface hydroxyl group on the silica walls is either neutral or cationic at acidic pH and therefore would not prefer adsorption of Cu^{2+}-GSH complex. Therefore, pH 6 was chosen for subsequent experiments.

Influence of scan rate on glutathione signal

In order to evaluate the mechanism of the complex oxidation, the influence of scan rate was investigated. Silica thin film modified electrode was immersed into 0.1 M KNO_3 with 22.0 µM glutathione and 35.0 µM Cu and cyclic voltammetry was carried out at scan rates of 0.02 to 0.6 V s^{-1}. As can be seen in Fig. 5, peak currents increased monotonically

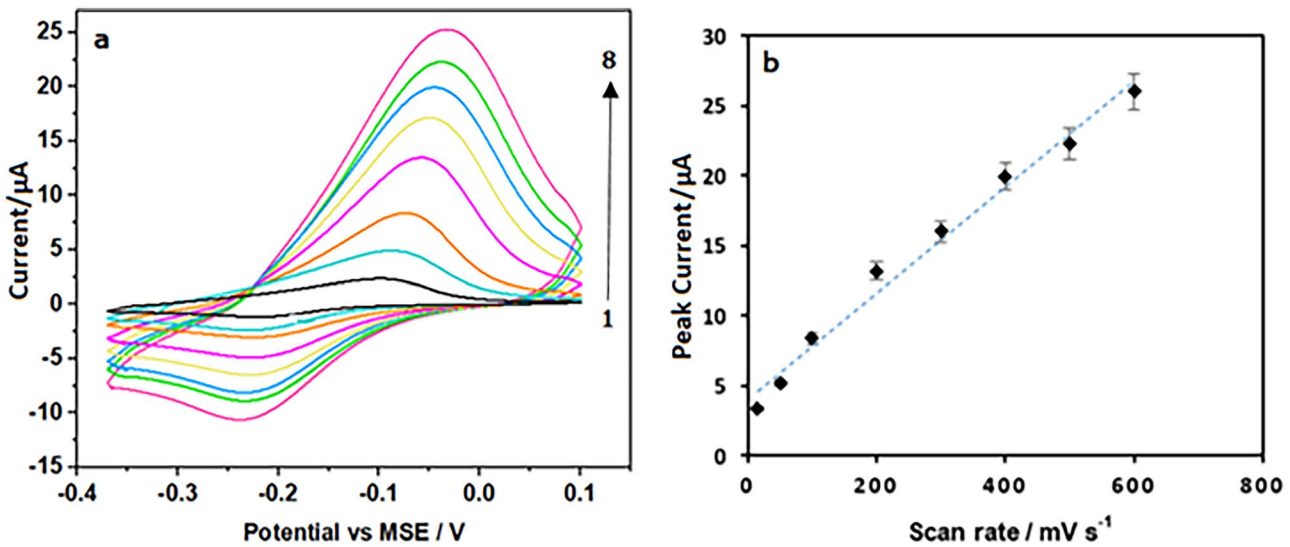

Fig. 5 **a** The cyclic voltammograms recorded of a MSTF/GC electrode in 0.1 M KNO_3 + 22.0 µM glutathione and + 35.0 µM Cu^{+2} at several scan rates of 20 (1), 50 (2), 100 (3), 200 (4), 300 (5), 400 (6), 500 (7), 600 (8) mV/s; **b** a plot of the Ip dependence on the scan rate

with the scan rate. Linear dependency of the peak current on the scan rate proposes adsorption-controlled process.

The surface coverage Γ (mol cm^{-2}) can be calculated in agreement with the Sharp equation as shown below [38] where the peak current depends on the surface concentration of $[Cu-SG]^+$ on the silica thin film modified GC electrode.

$$I_p = n^2F.^2A\Gamma v/4RT$$

In this equation, n describes the number of electrons participating in the reaction, A indicates the surface area of the modified electrode, and the other items have their typical meaning. The obtained results show that the surface coverage can be estimated from the slope of the anodic peak current plotted against the scan rate, which suggests that 7.6×10^{-10} mol cm^{-2} of Cu^{+2}-GSH complex compound can adsorb on the proposed electrode surface for $n=2$.

Calibration plot for glutathione oxidation in the presence of Cu^{2+}

In order to plot the calibration curve, cyclic voltammetry was studied with various concentrations of the GSH and 35.0 µM Cu^{+2} in 0.1 M KNO_3 solution. Figure 6a shows that the peak current increases with GSH concentration. The measured Ip is plotted versus the increasing glutathione concentration and a linear relationship appears in Fig. 6b. The calibration curve (the blue line) is plotted in the concentration domain varying from 1.0 to 35.0 µM for GSH. In addition, the detection limit was calculated at 0.08 µM according to the signal which amounted to 3 times the standard deviation of the blank signal divided by the slope of the regression equation. The linear dynamic range obtained from this method is in the range of physiological fluids reported in the literature for GSH (2.0 to 12.0 µM of glutathione) and indicates that the sample can be analyzed without additional dilution or preconcentration. This is important for industrial application and clinical analysis as it can reduce analysis time, cost, and chemical waste.

Reaction mechanism

As observed in Fig. 6, with the increase of GSH concentration up to 35.0 µM, the peak current increases. When the concentration of GSH exceeds the concentration of copper, the peak current becomes relatively stable and then decreases. Signal reduction may be attributed to the loss of silica structure when the film is saturated with the complex. This problem can be solved by depositing silica films with the help of APTES electrografting as a molecular glue to enable silica film adhere well to the glassy carbon electrode surface [28]. The intercept of the two extrapolated best-fit lines of the peak current against glutathione concentration (Fig. 6b) is placed at 38.0 µM, which is the result of the formation of a 1:1 complex [34] between Cu^{2+} and GSH ($[Cu-SG]^+$). Oxidation of this species on the electrode surface can be described by the following equation:

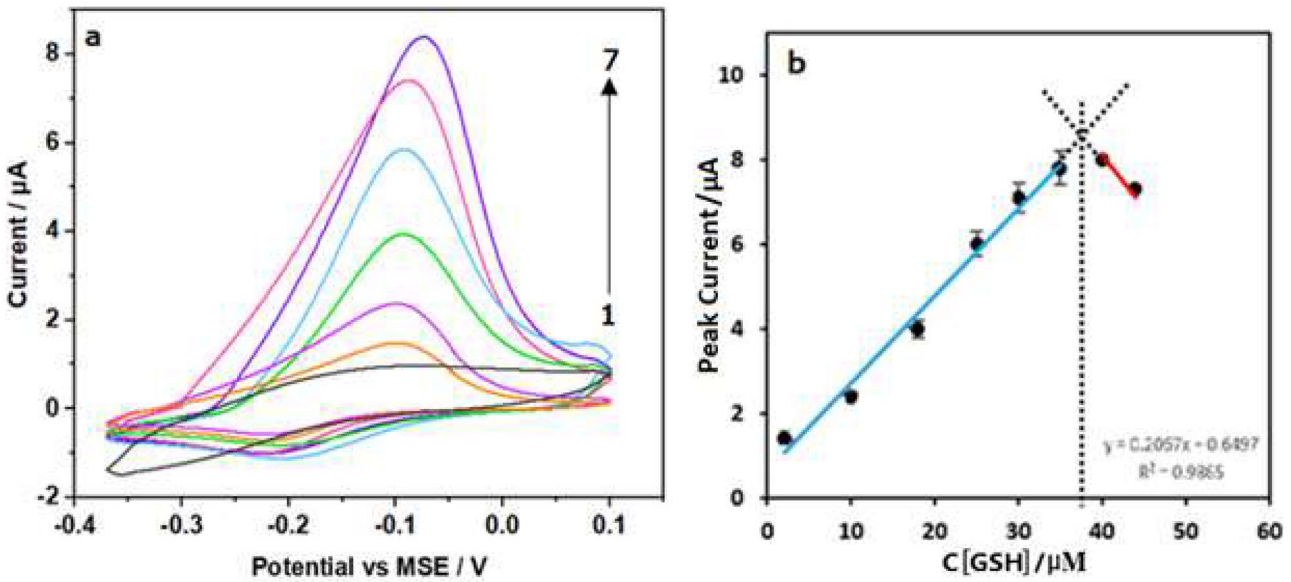

Fig. 6 a Cyclic voltammograms of a MSTF/GC electrode in 0.1 M KNO_3 solution (pH 6.0) using 35.0 µM of Cu^{+2} with GSH concentrations ranging of 0 (1); 1.0 (2); 10.0 (3); 20.0 (4); 25.0 (5); 30.0 (6); 35.0 µM (7). b The plot of peak current vs. concentration of the glutathione in the range from 1.0 to 35.0 µM, standard deviation for $n=3$. The red line is the best fit of data points achieved from GSH concentration range from 40.0 to 45.0 µM. The extrapolation of the two lines demonstrates that the stoichiometric ratio of the GSH (38.0 µM) to copper(II) is 1:1

$2[Cu-SG]^{+} \rightarrow Cu_2(GSSG) + 2e^{-}$

A higher ability to bind copper was obtained when thiol groups were present in the reduced form as it has been reported. Although, the binding is minimal when thiol groups are oxidized to disulfide bonds [39].

Determination of glutathione in the presence of cysteine

Some possible chemical interferences that are structurally related to GSH, such as cysteine that is present in yeast and blood, have also been tested [40–42]. Glutathione was measured by introducing cysteine into the system with the standard addition method. A mixture of equal concentrations of glutathione (8.0 µM) and cysteine (8.0 µM) was prepared and introduced into four standard solutions containing 7.0 to 16.0 µM glutathione standard and 35 µM of Cu^{+2} in 0.1 M KNO_3. The results showed that the increase in the anodic peak was related to the concentration of GSH and thus a linear relation between the concentration of the GSH standard and the peak current is recorded in Fig. 7a. Extrapolating to the zero current specified that 8.4 µM of glutathione is present as the analyte in the solution (Fig. 7b), which corresponds well to the initial value of the reagent (8.0 µM). Thus, the result shows cysteine does not seriously interfere with the sensor response.

Selectivity and reproducibility of GSH electrode

Selectivity is explained as the capability of an analytical method to precisely determine the GSH in the presence of other expected interfering substances such as glutamic acid, glucose, and ascorbic acid which have similar oxidation potential. For this purpose, the signal for a concentration of 10.0 µm GSH was obtained and the recorded signal was compared with the mixture of GSH and interfering compound in a 5:1 molar ratio. GSH recovery values are observed in the presence of interfering compounds in Table S1. The results displayed no interference on the electrode response, which exhibits high selectivity of the proposed sensor for GSH determination. In addition, the reproducibility of the sensor was assessed by measuring the CV peak currents of 3 different modified electrodes for a 22.0 µM GSH solution. The relative standard deviation (RSD) was 2.5%, indicating that the proposed sensor has desirable reproducibility. To investigate the stability of the proposed sensor, the MSTF-modified electrode before template extraction was maintained at room temperature for 1 month. The results showed that the corresponding CV peak current decreased only by 2.1% of its initial current, suggesting a good measurement stability.

GSH determination in real sample

Glutathione was determined successfully in several serum samples by using the mesoporous silica thin film–GC electrode. For this purpose, the blood samples were first centrifuged for 15 min at 3000 rpm to separate human serum. In this step, 30.0 µL of human serum was diluted to 3.0 mL in 0.1 M KNO_3 solution, and then various concentrations of GSH were spiked to 1 mL of the diluted samples. As shown in Table 2, the recoveries and RSDs are in the range of 98.6–105.5% and 1.2–2.2%, respectively, suggesting the proposed sensor has good reliability in the determination of real sample.

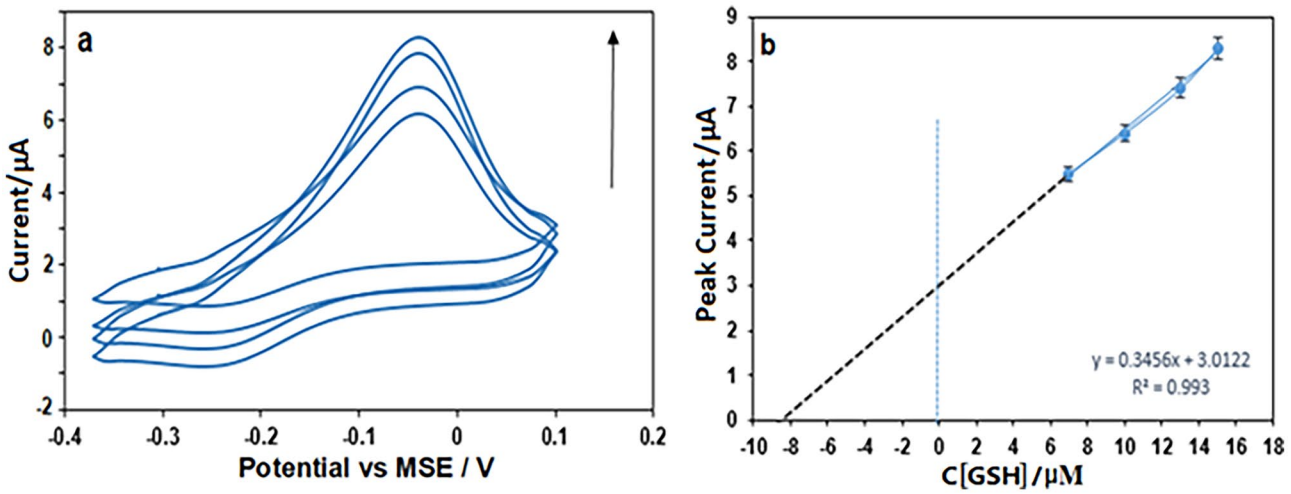

Fig. 7 **a** Cyclic voltammograms of a MSTF/GC electrode studied in 0.1 M KNO_3 solution (pH 6.0) containing 35.0 µM of Cu^{+2} with various GSH concentrations ranging of 7.0, 10.0, 13.0, and 16.0 µM in presence of 8.0 µM glutathione + 8.0 µM cysteine at 50 mV s^{-1}. **b** The blue line as a function of the standard GSH concentration is the best fit of data between 7.0 and 16.0 µM

Table 2 Recovery results of MSTF/GC electrode by standard addition method for glutathione detection in 0.1 M KNO_3 solution at pH 6.0 using 35.0 µM of Cu^{+2} ($n = 3$)

Sample	Added (µM)	Found (µM)	RSD (%)	Recovery (%)
1	10	10.3	2.2	103
2	20	21.1	1.6	105.5
3	30	29.6	1.2	98.6

Conclusions

An organic monolayer of the mesoporous silica-based thin film was deposited at the GC electrode surface for the rapid and simple oxidation of glutathione mediated by copper. Compared with the other chemically modified electrodes, the preparation of silica film via electrochemically assisted self-assembly (EASA) technique is a one quick step process and very simple in design, providing good stability for silica films on the GC electrode. Such silica films provide an excellent fixation site, increasing the surface area to increase the number of reactive sites, and therefore increasing the signal-to-noise ratio and also decreasing surface passivation. The current signal is detected at a low oxidation potential of − 0.10 V (vs. MSE) that markedly lowered the overpotential for GSH oxidation and makes the proposed sensor applicable to minimize interference. Therefore, this method is particularly important for clinical analysis and laboratory application.

Supplementary Information The online version contains supplementary material available at https://doi.org/10.1007/s10008-022-05234-7.

Funding The authors received financial support from the Yazd University Research Council.

References

1. Forman HJ, Zhang H, Rinna A (2009) Glutathione: overview of its protective roles, measurement, and biosynthesis. Mol Aspects Med 30:1–12
2. Ames BN (1983) Dietary carcinogens and anticarcinogens: oxygen radicals and degenerative diseases. Science 221:1256–1264
3. Cerutti PA (1985) Prooxidant states and tumor promotion. Science 227:375–381
4. Goodman MT, McDuffie K, Hernandez B, Wilkens LR, Selhub J (2000) Case-control study of plasma folate, homocysteine, vitamin B12, and cysteine as markers of cervical dysplasia. American Cancer Society 89:376–382
5. Buhl R, Holroyd K, Mastrangeli A, Cantin A, Jaffe HA, Wells F, Saltini C, Crystal R (1989) Systemic glutathione deficiency in symptom-free HIV-seropositive individuals. Lancet 334:1294–1298
6. Pastore A, Piemonte F, Locatelli M, Russo AL, Gaeta LM, Tozzi G, Federici G (2001) Determination of blood total, reduced, and oxidized glutathione in pediatric subjects. Clin Chem 47:1467–1469
7. Halprin KM, Ohkawara A (1967) The measurement of glutathione in human epidermis using glutathione reductase. J invest dermatol 48:149–152
8. Morel Y, Barouki R (1999) Repression of gene expression by oxidative stress. Biochemical Journal 342:481–496
9. Kleinman WA, Richie JP Jr (2000) Status of glutathione and other thiols and disulfides in human plasma. Biochem Pharmacol 60:19–29
10. Dröge W, Breitkreutz R (2000) Glutathione and immune function. Proc Nutr Soc 59:595–600
11. Helbling B, Von Overbeck J, Lauterburg B (1996) Decreased release of glutathione into the systemic circulation of patients with HIV infection. EJCI 26:38–44
12. Rossi R, Dalle-Donne I, Milzani A, Giustarini D (2006) Oxidized forms of glutathione in peripheral blood as biomarkers of oxidative stress. Clin Chem 52:1406–1414
13. Pozdeev V, Pozdeyev N (2010) Determination of total aminothiols and neuroactive amino acids in plasma by high performance liquid chromatography with fluorescence detection. Biochem (Mosc) Suppl B: Biomed Chem 4:288–295
14. Parmentier C, Wellman M, Nicolas A, Siest G, Leroy P (1999) Simultaneous measurement of reactive oxygen species and reduced glutathione using capillary electrophoresis and laser-induced fluorescence detection in cultured cell lines. Electrophoresis: An Int J 20:2938–2944
15. Carru C, Zinellu A, Mario Pes G, Marongiu G, Tadolini B, Deiana L (2002) Ultrarapid capillary electrophoresis method for the determination of reduced and oxidized glutathione in red blood cells. Electrophoresis 23:1716–1721
16. Su W-Y, Cheng S-H (2008) Electrocatalysis and sensitive determination of cysteine at poly (3, 4-ethylenedioxythiophene)-modified screen-printed electrodes. Electrochem commun 10:899–902
17. Harfield JC, Batchelor-McAuley C, Compton RG (2012) Electrochemical determination of glutathione: a review. Analyst 137:2285–2296
18. Lee PT, Goncalves LM, Compton RG (2015) Electrochemical determination of free and total glutathione in human saliva samples. Sens Actuators B Chem 221:962–968
19. Zaidi SA, Shin JH (2016) A review on the latest developments in nanostructure-based electrochemical sensors for glutathione. Anal Methods 8:1745–1754
20. Mazloum-Ardakani M, Sheikh-Mohseni MA, Mirjalili BF (2013) Selective and simultaneous voltammetric determination of glutathione, uric acid and penicillamine by a modified carbon nanotube paste electrode. Electroanalysis 25:2021–2029
21. Ralph T, Hitchman M, Millington J, Walsh F (1994) The electrochemistry of L-cystine and L-cysteine: part 1: thermodynamic and kinetic studies. J Electroanal Chem 375:1–15
22. Walcarius A (2018) Silica-based electrochemical sensors and biosensors: recent trends. Curr Opin Electrochem 10:88–97
23. Argoubi W, Sanchez A, Parrado C, Raouafi N, Villalonga R (2018) Label-free electrochemical aptasensing platform based on mesoporous silica thin film for the detection of prostate specific antigen. Sens Actuators B Chem 255:309–315
24. Nasir T, Herzog G, g, Hébrant M, Despas C, Liu L, Walcarius A, (2018) Mesoporous silica thin films for improved electrochemical detection of paraquat. ACS sensors 3:484–493
25. Walcarius A, Sibottier E, Etienne M, Ghanbaja J (2007) Electrochemically assisted self-assembly of mesoporous silica thin films. Nat Mater 6:602–608
26. Walcarius A (2013) Mesoporous materials and electrochemistry. Chem Soc Rev 42:4098–4140
27. Salimi A, Pourbeyram S (2003) Renewable sol–gel carbon ceramic electrodes modified with a Ru-complex for the amperometric detection of l-cysteine and glutathione. Talanta 60:205–214
28. Asadpour F, Mazloum-Ardakani M, Hoseynidokht F, Moshtaghioun SM (2021) In situ monitoring of gating approach on mesoporous

silica nanoparticles thin-film generated by the EASA method for electrochemical detection of insulin. Biosens Bioelectron 180:113124
29. Nasir T, Herzog G, Hébrant M, Despas C, Liu L, Walcarius A (2018) Mesoporous silica thin films for improved electrochemical detection of paraquat. ACS Sens 3:484–493
30. Maria Chong A, Zhao X (2003) Functionalization of SBA-15 with APTES and characterization of functionalized materials. J Phys Chem B 107:12650–12657
31. White L, Tripp C (2000) Reaction of (3-aminopropyl) dimethylethoxysilane with amine catalysts on silica surfaces. J Colloid Interface Sci 232:400–407
32. Shakeri A, Razavi R, Salehi H, Fallahi M, Eghbalazar T (2019) Thin film nanocomposite forward osmosis membrane embedded with amine-functionalized ordered mesoporous silica. Appl Surf Sci 481:811–818
33. Cheng W, Compton RG (2016) Measuring the content of a single liposome through electrocatalytic nanoimpact "titrations." ChemElectroChem 3:2017–2020
34. Areias MC, Shimizu K, Compton RG (2016) Voltammetric detection of glutathione: an adsorptive stripping voltammetry approach. Analyst 141:2904–2910
35. Ngamchuea K, Batchelor-McAuley C, Compton R (2016) The copper (II)-catalyzed oxidation of glutathione. Eur J Chem 22
36. Huang H, Li H, Feng J-J, Feng H, Wang A-J, Qian Z (2017) One-pot green synthesis of highly fluorescent glutathione-stabilized copper nanoclusters for Fe3+ sensing. Sens Actuators B Chem 241:292–297
37. Hormozi-Nezhad M, Seyedhosseini E, Robatjazi H (2012) Spectrophotometric determination of glutathione and cysteine based on aggregation of colloidal gold nanoparticles. Sci Iran 19:958–963
38. Ardakani MM, Talebi A, Naeimi H, Barzoky MN, Taghavinia N (2009) Fabrication of modified TiO 2 nanoparticle carbon paste electrode for simultaneous determination of dopamine, uric acid, and l-cysteine. J Solid State Electrochem 13:1433–1440
39. Safavi A, Maleki N, Farjami E, Mahyari FA (2009) Simultaneous electrochemical determination of glutathione and glutathione disulfide at a nanoscale copper hydroxide composite carbon ionic liquid electrode. Anal Chem 81:7538–7543
40. Ardakani MM, Rahimi P, Karami PE, Zare HR, Naeimi H (2007) Electrocatalytic oxidation of cysteine by quinizarine at glassy carbon electrode. Sens Actuators, BCurrent BiologyChemistry & Biodiversity 123:763–768
41. Mazloum-Ardakani M, Alizadeh Z (2020) A certain electrochemical nanosensor based on functionalized multi-walled carbon nanotube for determination of cysteine in the presence of paracetamol. Journal of Nanostructures 10:258–267
42. Mazloum-Ardakani M, Taleat Z, Beitollahi H, Naeimi H (2010) Selective determination of cysteine in the presence of tryptophan by carbon paste electrode modified with quinizarine. J Iran Chem Soc 7:251–259
43. Mao L, Yamamoto K (2000) Amperometric biosensor for glutathione based on osmium-polyvinylpyridine gel polymer and glutathione sulfhydryl oxidase. Electroynalysis (N.Y.N.Y.) 12:577–582
44. Gong K, Zhu X, Zhao R, Xiong S, Mao L, Chen C (2005) Rational attachment of synthetic triptycene orthoquinone onto carbon nanotubes for electrocatalysis and sensitive detection of thiols. Anal Chem 77:8158–8165
45. Luz R, d CS, Damos FS, Gandra PG, de Macedo DV, Tanaka AA, Kubota LT (2007) Electrocatalytic determination of reduced glutathione in human erythrocytes. Anal Bioanal Chem 387:1891–1897
46. Mishra GK, Krishna V, Prakash R (2009) Synthesis and characterization of novel heterobinuclear mercury (II)-DTPA-M (II) complexes: electrocatalytic and sensor applications. Synth React Inorg Met Org Chem 39:124–128
47. Raoof J-B, Ojani R, Baghayeri M (2009) Simultaneous electrochemical determination of glutathione and tryptophan on a nano-TiO2/ferrocene carboxylic acid modified carbon paste electrode. Sens Actuators B Chem 143:261–269
48. Luz RC, Damos FS, Tanaka AA, Kubota LT, Gushikem Y (2008) Electrocatalysis of reduced L-glutathione oxidation by iron (III) tetra-(N-methyl-4-pyridyl)-porphyrin (FeT4MPyP) adsorbed on multi-walled carbon nanotubes. Talanta 76:1097–1104
49. Lee PT, Lowinsohn D, Compton RG (2014) The use of screen-printed electrodes in a proof of concept electrochemical estimation of homocysteine and glutathione in the presence of cysteine using catechol. Sensors 14:10395–10411
50. Raoof J, Ojani R, Karimi-Maleh H (2009) Electrocatalytic oxidation of glutathione at carbon paste electrode modified with 2, 7-bis (ferrocenyl ethyl) fluoren-9-one: application as a voltammetric sensor. J Appl Electrochem 39:1169–1175
51. Chen J, He Z, Liu H, Cha C (2006) Electrochemical determination of reduced glutathione (GSH) by applying the powder microelectrode technique. J Electroanal Chem 588:324–330
52. Li Y, Yang SY, Chen SM (2011) Biosensing approach for glutathione detection using glutathione reductase (GR) with multi-walled carbon nanotubes on gold electrode. Int J Electrochem Sci 6:3982–3996
53. Ricci F, Arduini F, Tuta CS, Sozzo U, Moscone D, Amine A, Palleschi G (2006) Glutathione amperometric detection based on a thiol–disulfide exchange reaction. Anal Chim Acta 558:164–170
54. Calvo-Marzal P, Chumbimuni-Torres KY, Höehr NF, Kubota LT (2006) Determination of glutathione in hemolysed erythrocyte with amperometric sensor based on TTF-TCNQ. Clin Chim Acta 371:152–158